Editors' Suggestion

Loss-Tolerant Detection of Squeezed States in the 2 μm Region

K. M. Kwan,[1,*] T. G. McRae,[1] J. Qin,[1] D. W. Gould,[1] S. S. Y. Chua,[1] J. Junker,[1,2] R. Iden,[3] V. B. Adya,[4] M. J. Yap,[1] B. J. J. Slagmolen,[1] D. E. McClelland,[1] and R. L. Ward[1]

[1]*OzGrav, Centre for Gravitational Astrophysics, Research School of Physics and Research School of Astronomy and Astrophysics, Australian National University, Australian Capital Territory, Australia*

[2]*Center for Macroscopic Quantum States (bigQ), Department of Physics, Technical University of Denmark, 2800 Kongens Lyngby, Denmark*

[3]*Institute of Science Tokyo, Tokyo, Japan*

[4]*Nonlinear and Quantum Photonics Lab, Department of Applied Physics, KTH Royal Institute of Technology, Stockholm, Sweden*

(Received 29 September 2025; revised 5 January 2026; accepted 17 February 2026; published 23 March 2026)

Squeezed states of light enable quantum-enhanced measurements but are limited by optical loss, particularly at 2 μm where photodiode efficiency is low. We report the first loss-tolerant, audio-band squeezed light detection at 1984 nm by using a phase-sensitive amplifier to amplify the squeezed vacuum prior to detection. This technique increases the effective detection efficiency from 74% to 95% and increases the observed squeezing from 4 to 8 dB, the highest level of squeezing observation reported at this wavelength. Additionally, the vacuum to dark-noise clearance increases, extending the effective measurement bandwidth toward lower frequencies. This approach is largely wavelength independent, extending high-fidelity quantum measurements to future gravitational-wave detectors and related quantum technologies.

DOI: 10.1103/s61z-fcyp

Introduction—Squeezed states of light enhance sensitivity in a range of precision measurements, including gravitational wave (GW) detection [1–7], biosensing [8], and quantum information [9]. Their practical utility, however, is limited by photon loss which degrades observable squeezing by introducing vacuum fluctuations and technical noise that masks the quantum correlations. While noises such as phase noise and photodiode dark noise affect all frequencies, their impact is especially pronounced in the audio band, which is relevant to GW detection [10,11].

The transition to a wavelength near 2 μm in proposed future GW detectors is motivated by thermal noise reduction [12–14]. These future detectors will employ cryogenic silicon test masses [15], that have high optical absorption at 1064 nm. At 1064 nm, up to 15 dB of tabletop squeezing has been demonstrated [16], compared to 4 dB at 1984 nm [17]. Squeezing has been integrated in the kilometer-scale interferometers [3], however loss and low-frequency detection remain major technical challenges.

The transition to the 2 μm wavelength introduces new difficulties. Although 2 μm photodiodes reach quantum efficiencies as high as 92% at MHz frequencies [18], photodetectors optimized for the audio band currently achieve only 74% [17]. Reverse biasing a photodiode can improve efficiency at the expense of increased dark noise; cryogenic cooling reduces dark noise but degrades quantum efficiency [19]. In contrast, current GW detectors at 1064 nm routinely exceed 98% efficiency [3,16]. Thus, achieving high-fidelity, audio-band squeezing at 2 μm remains a key technical hurdle for future detectors. To address the limitation of photodiode efficiency, we experimentally demonstrate quantum-enhanced detection at 1984 nm using a phase-sensitive amplifier to mitigate the impact of low photodiode efficiency. First proposed by Caves [20,21] this approach simultaneously amplifies the vacuum state, and any squeezed state, in the measurement quadrature above the Heisenberg limit. Both amplified states are affected by the loss, however, the degradation in the measured level of squeezing is less than with direct squeezed light detection, provided both amplified states remain above the Heisenberg limit. Proof-of-principle experiments have validated its loss-tolerant properties [22–24], and integrated photonics have demonstrated broadband, room-temperature implementations [9,25–28].

In the context of GW detectors, this technique underpins internal squeezing, where *in situ* amplification improves readout sensitivity [29]. Both theoretical and experimental work show that operating in the amplification regime can surpass the standard sensitivity-bandwidth limit [30–34]. For a force-sensing interferometer such as a GW detector, an output optical parametric amplifier (OPA), similar to the one described here, would amplify both the gravitational wave signal and the reflected squeezed vacuum at the interferometer output. These developments form the basis for our demonstration of loss-tolerant quantum sensing at 2 μm.

In this Letter, we demonstrate a loss and phase-noise tolerant measurement scheme that enhances detection in the

*Contact author: kar.kwan@anu.edu.au

presence of limiting dark noise. By externally amplifying squeezed vacuum at 1984 nm, we recover the squeezing degraded by low detector efficiency. Our results agree well with the model and validate the effective efficiency metric introduced to quantify detection performance [35]. Crucially, phase noise from the OPA has a negligible effect on observed squeezing, even at low frequencies. These findings establish a viable, loss-tolerant strategy for quantum-enhanced detection at 2 μm—directly applicable to next-generation GW observatories.

Experiments—The conceptual diagram for the squeezed vacuum generation and amplifier measurement setup is illustrated in Fig. 1(a). A subthreshold optical parametric oscillator (OPO) with an escape efficiency η_{opo} is used to generate the squeezed vacuum. Before reaching the OPA, the squeezing encounters propagation loss, η_{prop}, which in our setup is primarily due to mode mismatch between the two optical cavities. The squeezed vacuum is then amplified by an OPA that has escape efficiency η_{opa}. All losses after the OPA, including those due to diode quantum inefficiency, are characterized by the photodetection loss η_{det}.

Figure 1(b) shows a simplified layout of the experimental implementation. The OPO and OPA are dual-resonant bow-tie cavities with an identical design, as described in [17], with the input coupler reflectivity changed to 97% to reduce the threshold power for each cavity. A 1984 nm thulium fiber laser from AdValue Photonics [36] is used to provide a local oscillator (LO) for homodyne detection and

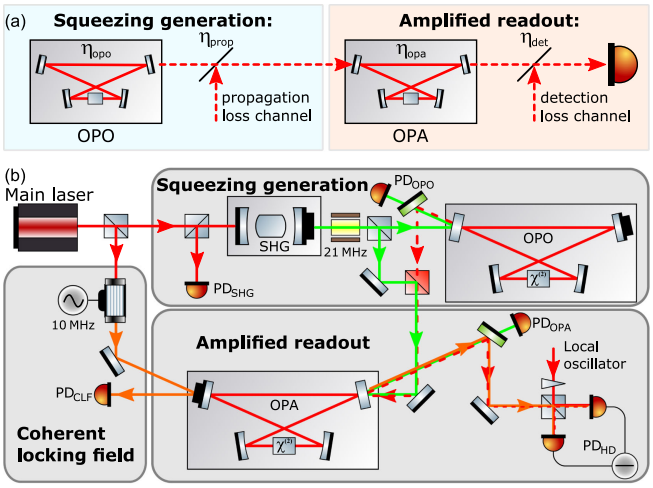

FIG. 1. (a) The nomenclature for the experimental setup and the vacuum coupled into the system as loss at key points. (b) The schematic for the experiment. The squeezed vacuum is generated from a squeezing setup that consists of a SHG and an OPO. The amplified readout consists of an OPA and a balanced homodyne detector. The photodiodes (PD) indicated are employed in the feedback loops. The 21 MHz sideband is used for PDH locking of OPO and OPA cavities. The 10 MHz CLF is used to control the pump phase of the OPA, shown as a single AOM for simplicity. The LO, split off from the main laser, is constrained to 150 μW to avoid the photodetector saturation.

to pump a second harmonic generator (SHG). The SHG is a periodically poled potassium titanyl phosphate (PPKTP) crystal placed in a 33 mm Fabry-Perot cavity that is stabilized on reflection with the Hansch-Couillaud method [37]. The pump field is split into two paths to pump the OPO and OPA. These cavities were Pound-Drever-Hall (PDH) locked to the pump with a phase modulation of 21 MHz. To control the pump phase of the OPA, we use the coherent locking field (CLF) technique where we inject a weak frequency-shifted field into the OPA [38–40]. The CLF 10 MHz frequency shift is generated from two acousto-optic modulators (AOM)'s (shown as one in Fig. 1) and is used to control the phase of the light relative to the OPA [41]. The LO is locked to the CLF using an error signal generated from the homodyne signal. This allows us to control the phase of the amplified readout scheme before injecting the squeezed vacuum into the OPA.

Characterizing the OPO and the OPA—We measure the squeezing generated separately by the OPO and OPA to characterize the phase noise and the photodetector loss. For the OPO squeezing measurement, the OPA is bypassed. These squeezing measurements (not shown) allow a measurement of total loss and phase noise in our setup. The squeezing-antisqueezing variance $(V_{(\mp)})$ is given by

$$V_{(\mp)} = 1 \mp \frac{4x\eta_{\mathrm{tot}}}{(1 \pm x)^2}, \tag{1}$$

where $\eta_{\mathrm{tot}} = \eta_{\mathrm{opo}}\eta_{\mathrm{hd}}\eta_{\mathrm{det}}$ is the total efficiency of the setup. The normalized pump parameter x, often measured from the nonlinear gain G, is given by

$$x = \sqrt{\frac{P}{P_{\mathrm{thresh}}}} = 1 - \frac{1}{\sqrt{G}}, \tag{2}$$

where P is the pump power and P_{thresh} is the threshold pump power of the cavity.

The effect of phase noise on the squeezed state is given by

$$V_{(\mp)}(\theta_i) = V_{(\mp)}\cos^2\theta_i + V_{(\pm)}\sin^2\theta_i, \tag{3}$$

where $i \in \{\mathrm{opo}, \mathrm{opa}\}$. The characterized losses and phase noise are summarized in Table I.

These measurements show large amplifier phase noise between the homodyne detection angle and the OPA. This originates from the phase lock between the OPA's CLF and the local oscillator. Lower CLF power would reduce the OPA phase noise to (144 ± 16) mrad, at the expense of the lock stability, due to the limited signal-to-noise ratio of the 2 μm commercial photodetector. While such excess phase noise is detrimental to measurements in the squeezed quadrature, the OPA is operated under amplification, where the effect of phase noise is strongly suppressed. This effect has been modeled and verified in our previous work [35],

TABLE I. The experimental parameters.

Parameter	Value
Escape efficiency of OPO, η_{opo}	$(98.2 \pm 0.5)\%$
Escape efficiency of OPA, η_{opa}	$(97.3 \pm 0.5)\%$
Homodyne detector efficiency, η_{hd}	$(98 \pm 1)\%$
Other propagation loss	$< 1\%$
Mode match between OPO and OPA	$(97 \pm 1)\%$
Photodiode quantum efficiency, η_{det}	$(74 \pm 3)\%$
Squeezing phase noise (without OPA), θ_{opo}	(46 ± 4) mrad
Squeezing phase noise (with OPA), θ_{opo}	(33 ± 1) mrad
Amplifier phase noise, θ_{opa}	(218 ± 1) mrad

confirming that amplifier phase noise contributes negligibly in the amplification regime.

Amplified squeezing measurements—In our configuration, both the OPO and the OPA are operated without any coherent seed field. We are measuring the quadrature being amplified by the OPA while scanning the pump phase into the OPO. With the homodyne detector locked to the amplified quadrature we can operate the OPA at different levels of nonlinear gain and inject different levels of squeezed vacuum from the OPO.

Figure 2 shows the squeezing result for $G_{opo} = 10$ and $G_{opa} = 12$. Trace (i) shows the amplified squeezing, from the OPA, as the pump phase to the OPO is scanned through the squeezed and antisqueezed quadratures. Trace (ii) shows the corresponding amplified vacuum noise, sometimes referred to as amplified shot noise. Trace (iii) shows the vacuum noise without parametric amplification from the OPA measured by the homodyne detector with a local oscillator power of 150 μW. Trace (iv) shows the homodyne detector's dark noise. As the homodyne detector is locked to the OPA pump phase at the antisqueezed quadrature, the x-axis "time" is correlated to the relative phase of the squeezing from the OPO as we slowly scan the OPO pump phase. Without the OPA, the observed squeezing is limited to 4 dB with 26% of photodetection loss. With the OPA providing 14 dB of amplification, the observed squeezing increases to (8 ± 1) dB.

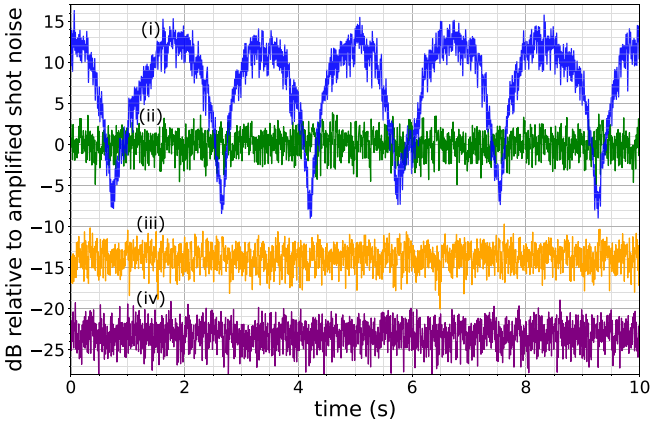

FIG. 2. Measurement of the amplified squeezing level normalized to the amplified vacuum noise centered at 52 kHz. Traces correspond to (i) amplified squeezing and antisqueezing, (ii) amplified vacuum noise, (iii) vacuum noise, and (iv) dark noise. The data are taken for $G_{opo} = 10$ and $G_{opa} = 12$, respectively. The zero span measurement was taken with a 1 kHz resolution bandwidth and 30 Hz video bandwidth.

Figure 3 shows the amplified squeezing and antisqueezing generated by the OPO for the OPA operating under three different gain conditions. We fit a squeezing phase noise of 33 mrad. The OPA with phase locking acts as a reference cavity for the OPO and reduces the squeezing phase noise. Although the characterization of the OPA exhibited relatively large amplification phase noise, our model predicts that 218 mrad of amplification phase noise would degrade the squeezing by less than 0.5 dB when $G_{opo} \approx G_{opa}$. Figure 3 demonstrates that amplified squeezing is largely insensitive to amplifier phase noise. In comparison, high squeezing phase noise when operating in the region of high nonlinear gain without an OPA can significantly degrade the measured level of squeezing.

Our previous work [35] shows that the amplified squeezing can be expressed as

$$V_{(-)}^{\mathrm{eff}} = \frac{V_{(-)}^{\mathrm{amp}}}{V_{(-)}^{\mathrm{amp}}|_{G_{opo}=1}} = 1 - \frac{4x_{\mathrm{opo}}\tilde{\eta}_{\mathrm{sqz}}\eta_{\mathrm{eff}}}{(1+x_{\mathrm{opo}})^2}. \tag{4}$$

This equation has the same form as Eq. (1), where $V_{(-)}^{\mathrm{amp}}$ is the amplified squeezing, $V_{(-)}^{\mathrm{amp}}|_{G_{opo}=1}$ is the amplified vacuum noise, and η_{eff} is given by

$$\eta_{\mathrm{eff}} = \frac{\eta_{\mathrm{det}}(2\eta_{\mathrm{opa}} + x_{\mathrm{opa}} - 1)^2}{(1-x_{\mathrm{opa}})^2 + 4x_{\mathrm{opa}}\eta_{\mathrm{det}}\eta_{\mathrm{opa}}}. \tag{5}$$

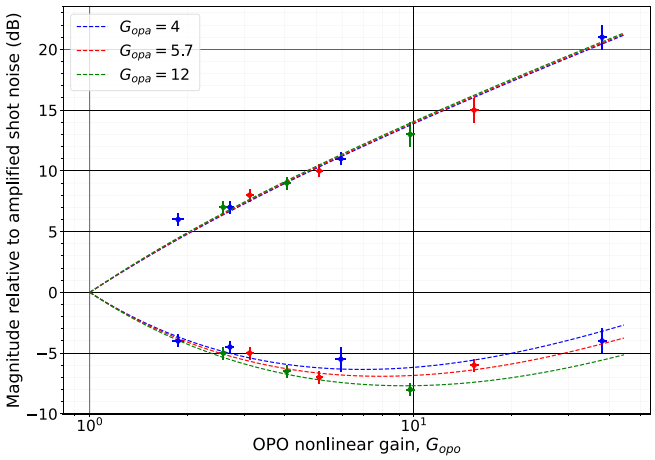

FIG. 3. Amplified antisqueezing and squeezing operating versus the OPO nonlinear gain, with photodetector efficiency of 74% and OPA operating at nonlinear gain of 4 (blue), 5.7 (red), and 12 (green).

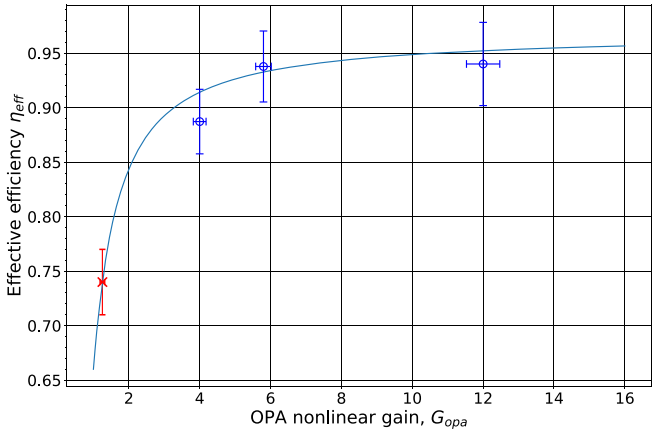

FIG. 4. Enhanced effective efficiency versus OPA nonlinear gain. Measured efficiencies are plotted as circles at each gain. The threshold gain where internal OPA loss is exactly compensated is marked by a red cross.

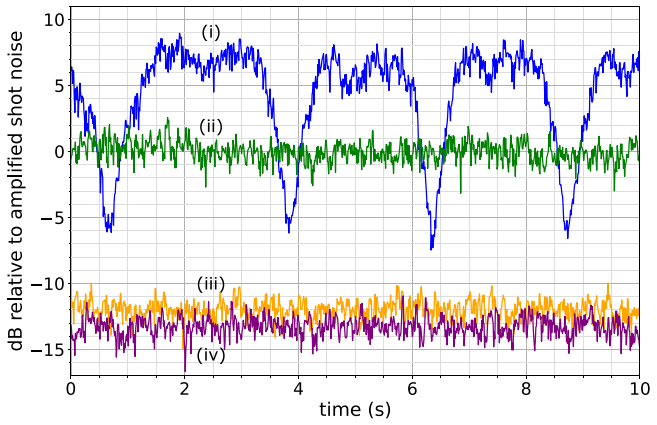

FIG. 5. Measurement of the amplified squeezing at $G_{\mathrm{opo}} = 3$ at 3 kHz. The traces correspond to (i) amplified squeezing and antisqueezing, (ii) amplified vacuum noise, (iii) vacuum noise, and (iv) dark noise. The additional noise clearance is obtained from $G_{\mathrm{opa}} = 19$. The zero span measurement was taken with a 1 kHz resolution bandwidth and 10 Hz video bandwidth.

Here, we separate the efficiency terms into the efficiency of squeezing generation $\tilde{\eta}_{\mathrm{sqz}} = \eta_{\mathrm{opo}}\eta_{\mathrm{prop}}$ and the effective efficiency of the amplified readout η_{eff} described by Eq. (5). The effective efficiency, representing the amplified readout efficiency shown in Fig. 1, is primarily tuned by varying the nonlinear gain of OPA.

Figure 4 shows the enhanced efficiency of our measurement system as a function of OPA nonlinear gain. We obtained the effective efficiency η_{eff} from our amplified squeezing and antisqueezing results. The error bars for the data points in Fig. 4 are estimated from the fitting parameters of Fig. 3. A theoretical curve is included in Fig. 4 that is calculated from experimentally measured parameters such as photodiode quantum efficiency and OPA escape efficiency (Table I). Figure 4 shows the increase in efficiency corresponding to the increase in OPA nonlinear gain. The graph is plotted with the fitted η_{eff}, and the η_{eff} calculated from measured η_{opa}, η_{det}, and x_{opa} values.

We obtain the expression for the minimum pump required to compensate for OPA internal loss x_{int} that can be written as

$$x_{\mathrm{int}} = \frac{1-\eta_{\mathrm{opa}}}{1-\eta_{\mathrm{det}}} = \frac{L_{\mathrm{opa}}}{L_{\mathrm{det}}}, \tag{6}$$

where L_{opa} is the intracavity loss of the OPA and L_{det} is the photodetection loss. This expression is obtained by setting $\eta_{\mathrm{eff}} = \eta_{\mathrm{det}}$ in Eq. (5). Without amplification from the OPA ($G_{\mathrm{opa}} = 1$), the overall efficiency is degraded due to the additional intracavity loss introduced by the OPA. In our measurement setup, the OPA requires a nonlinear gain of 1.25 to compensate for the 2.7% intracavity loss introduced by the amplifier highlighted with the red cross on Fig. 4. The upper limit for the amplified readout scheme is set by x_{int}, where a lossless OPA ($x_{\mathrm{int}} = 0$) is required to achieve $\eta_{\mathrm{eff}} = 1$. With a modestly high gain ($G_{\mathrm{opa}} > 10$), we were able to achieve an efficiency of 95% with our OPA.

The reduction of technical noise such as electronic noise or photodiode dark noise is important at low frequencies for applications such as GW detection where high levels of squeezing are essential. As shown in Fig. 5, at 3 kHz the noise clearance is reduced to 1 dB, where the limiting noise source originates from the electronic noise floor of the spectrum analyzer rather than from the photodiode. Conventional detection schemes typically require more than 10 dB of clearance to observe squeezing. By contrast, the OPA adds 12 dB of noise clearance, enabling the observation 6.5 dB of squeezing in the noise-limited region. While the noise limitation here is electronic rather than from the photodiode, the same principle still holds, where phase-sensitive amplification extends the bandwidth of measurement systems.

The bandwidth, with its upper limit set by the OPA cavity linewidth, is especially valuable when the LO power is limited, where further increase in LO power can couple additional technical noise such as relative intensity noise (RIN) or Johnson noise from heating of the photodiode, limiting the observed squeezing. In this regime, some sources of dark noise, such as flicker noise that scales with $1/f$, are not well understood. By amplifying vacuum noise, the OPA can potentially mitigate the limitation of the photodiode's semiconductor properties.

Conclusions and discussions—We observed 8 dB of squeezing in 2 μm region with photodiodes that have a quantum efficiency of 74%. This experiment demonstrates an alternative wavelength-independent technique to achieve high detection efficiency. At 2 μm, we demonstrate an effective detection efficiency of 95%, among the highest reported, while extending the bandwidth into the dark-noise-dominated low frequency region. Although lower intracavity losses have been achieved, developing a photodetector with an equivalent loss figure presents a much

greater challenge at this wavelength. With an OPA that has an escape efficiency of 99% [16], we could improve the efficiency of the measurement scheme to 98%, a level comparable to the photodiodes currently used in GW detectors. We have shown that phase noise in the OPA has a minimal effect on the observation of squeezing. In addition, this technique allows amplification above dark noise in the regime limited by semiconductor properties.

Acknowledgments—This research was supported by the Australian Research Council under the ARC Centre of Excellence for Gravitational Wave Discovery, Grant No. CE230100016. R. I. would like to acknowledge the support and funding from JST ASPIRE, Grant No. JPMJAP2320. V. B. A. would like to acknowledge the support and funding from the Swedish Research Council (VR starting Grant No. 2023-0519, the Wallenberg Center for Quantum Technology (WACQT) and the Göran Gustafsson Foundation in Sweden. This work has been assigned LIGO document number P2500501.

The authors declare no competing interests.

Data availability—The data that support the findings of this article are not publicly available upon publication because it is not technically feasible and/or the cost of preparing, depositing, and hosting the data would be prohibitive within the terms of this research project. The data are available from the authors upon reasonable request.

[1] J. Abadie, B. P. Abbott, R. Abbott, T. D. Abbott, M. Abernathy, C. Adams, R. Adhikari, C. Affeldt, B. Allen, G. S. Allen *et al.* (The LIGO Scientific Collaboration), Nat. Phys. **7**, 962 (2011).
[2] F. Acernese, M. Agathos, L. Aiello, A. Allocca, A. Amato, S. Ansoldi, S. Antier, M. Arène, N. Arnaud, S. Ascenzi *et al.* (Virgo Collaboration), Phys. Rev. Lett. **123**, 231108 (2019).
[3] M. Tse, H. Yu, N. Kijbunchoo, A. Fernandez-Galiana, P. Dupej, L. Barsotti, C. D. Blair, D. D. Brown, S. E. Dwyer, A. Effler *et al.*, Phys. Rev. Lett. **123**, 231107 (2019).
[4] J. Aasi, J. Abadie, B. P. Abbott, R. Abbott, T. D. Abbott, M. R. Abernathy, C. Adams, T. Adams, P. Addesso, R. X. Adhikari *et al.*, Nat. Photonics **7**, 613 (2013).
[5] H. Yu, L. McCuller, M. Tse, N. Kijbunchoo, L. Barsotti, N. Mavalvala, J. Betzwieser, C. D. Blair, S. E. Dwyer, A. Effler *et al.* (The LIGO Scientific Collaboration), Nature (London) **583**, 43 (2020).
[6] J. Lough, E. Schreiber, F. Bergamin, H. Grote, M. Mehmet, H. Vahlbruch, C. Affeldt, M. Brinkmann, A. Bisht, V. Kringel *et al.*, Phys. Rev. Lett. **126**, 041102 (2021).
[7] M. J. Yap, J. Cripe, G. L. Mansell, T. G. McRae, R. L. Ward, B. J. J. Slagmolen, P. Heu, D. Follman, G. D. Cole, T. Corbitt, and D. E. McClelland, Nat. Photonics **14**, 19 (2020).
[8] C. A. Casacio, L. S. Madsen, A. Terrasson, M. Waleed, K. Barnscheidt, B. Hage, M. A. Taylor, and W. P. Bowen, Nature (London) **594**, 201 (2021).
[9] N. Takanashi, A. Inoue, T. Kashiwazaki, T. Kazama, K. Enbutsu, R. Kasahara, T. Umeki, and A. Furusawa, Opt. Express **28**, 34916 (2020).
[10] S. Dwyer, L. Barsotti, S. S. Y. Chua, M. Evans, M. Factourovich, D. Gustafson, T. Isogai, K. Kawabe, A. Khalaidovski, P. K. Lam *et al.*, Opt. Express **21**, 19047 (2013).
[11] S. E. Dwyer, Quantum noise reduction using squeezed states in LIGO, Ph.D. thesis, Massachusetts Institute of Technology, 2013.
[12] R. X. Adhikari, K. Arai, A. F. Brooks, C. Wipf, O. Aguiar, P. Altin, B. Barr, L. Barsotti, R. Bassiri, A. Bell *et al.*, Classical Quantum Gravity **37**, 165003 (2020).
[13] K. Ackley, V. B. Adya, P. Agrawal, P. Altin, G. Ashton, M. Bailes, E. Baltinas, A. Barbuio, D. Beniwal, C. Blair *et al.*, Pub. Astron. Soc. Aust. **37**, e047 (2020).
[14] M. Maggiore, C. V. D. Broeck, N. Bartolo, E. Belgacem, D. Bertacca, M. A. Bizouard, M. Branchesi, S. Clesse, S. Foffa, J. García-Bellido *et al.*, J. Cosmol. Astropart. Phys. 03 (2020) 050.
[15] J. Eichholz, N. A. Holland, V. B. Adya, J. V. van Heijningen, R. L. Ward, B. J. J. Slagmolen, D. E. McClelland, and D. J. Ottaway, Phys. Rev. D **102**, 122003 (2020).
[16] H. Vahlbruch, M. Mehmet, K. Danzmann, and R. Schnabel, Phys. Rev. Lett. **117**, 110801 (2016).
[17] G. L. Mansell, T. G. McRae, P. A. Altin, M. J. Yap, R. L. Ward, B. J. J. Slagmolen, D. A. Shaddock, and D. E. McClelland, Phys. Rev. Lett. **120**, 203603 (2018).
[18] C. Darsow-Fromm, J. Gurs, R. Schnabel, and S. Steinlechner, Opt. Lett. **46**, 5850 (2021).
[19] J. Gurs, N. Sultmann, C. Darsow-Fromm, S. Steinlechner, and R. Schnabel, C.R. Phys. **27**, 41 (2025).
[20] C. M. Caves, Phys. Rev. D **23**, 1693 (1981).
[21] C. M. Caves, Phys. Rev. D **26**, 1817 (1982).
[22] M. Manceau, G. Leuchs, F. Khalili, and M. Chekhova, Phys. Rev. Lett. **119**, 223604 (2017).
[23] Y. Shaked, Y. Michael, R. Z. Vered, L. Bello, M. Rosenbluh, and A. Pe'er, Nat. Commun. **9**, 609 (2018).
[24] M. Malnou, D. A. Palken, B. M. Brubaker, L. R. Vale, G. C. Hilton, and K. W. Lehnert, Phys. Rev. X **9**, 021023 (2019).
[25] R. Nehra, R. Sekine, L. Ledezma, Q. Guo, R. M. Gray, A. Roy, and A. Marandi, Science **377**, 1333 (2022).
[26] J. Williams, E. Sendonaris, R. Nehra, R. M. Gray, R. Sekine, L. Ledezma, and A. Marandi, Phys. Rev. Res. **7**, 043006 (2025).
[27] T. Yamashima, T. Kashiwazaki, T. Suzuki, R. Nehra, T. Nakamura, A. Inoue, T. Umeki, K. Takase, W. Asavanant, M. Endo *et al.*, Opt. Express **33**, 5769 (2025).
[28] E. Sendonaris, J. Williams, R. Nehra, R. Gray, R. Sekine, L. Ledezma, and A. Marandi, arXiv:2410.18397.
[29] Z. Y. Ou, Phys. Rev. A **85**, 023815 (2012).
[30] V. B. Adya, M. J. Yap, D. Töyrä, T. G. McRae, P. A. Altin, L. K. Sarre, M. Meijerink, N. Kijbunchoo, B. J. J. Slagmolen, R. L. Ward, and D. E. McClelland, Classical Quantum Gravity **37**, 07LT02 (2020).
[31] K. Somiya, K. Suzuki, S. Otabe, and K. Harada, Phys. Rev. D **107**, 122005 (2023).
[32] K. Somiya, Y. Kataoka, J. Kato, N. Saito, and K. Yano, Phys. Lett. A **380**, 521 (2016).

[33] M. Korobko, Y. Ma, Y. Chen, and R. Schnabel, Light Sci. Appl. **8**, 118 (2019).
[34] M. Korobko, J. Südbeck, S. Steinlechner, and R. Schnabel, Phys. Rev. Lett. **131**, 143603 (2023).
[35] K. M. Kwan, M. J. Yap, J. Qin, D. W. Gould, S. S. Y. Chua, J. Junker, V. B. Adya, T. G. McRae, B. J. J. Slagmolen, and D. E. McClelland, Classical Quantum Gravity **41**, 215005 (2024).
[36] AdValue Photonics, Inc., *AP-SF Specification Sheet: 2um Single-Frequency Fiber Laser Seed* (AdValue Photonics, Inc., Tucson, AZ, USA 2022).
[37] T. Hansch and B. Couillaud, Opt. Commun. **35**, 441 (1980).
[38] M. J. Yap, D. W. Gould, T. G. McRae, P. A. Altin, N. Kijbunchoo, G. L. Mansell, R. L. Ward, D. A. Shaddock, B. J. J. Slagmolen, and D. E. McClelland, Opt. Lett. **44**, 5386 (2019).
[39] H. Vahlbruch, S. Chelkowski, B. Hage, A. Franzen, K. Danzmann, and R. Schnabel, Phys. Rev. Lett. **97**, 011101 (2006).
[40] S. Chelkowski, H. Vahlbruch, K. Danzmann, and R. Schnabel, Phys. Rev. A **75**, 043814 (2007).
[41] E. Oelker, G. Mansell, M. Tse, J. Miller, F. Matichard, L. Barsotti, P. Fritschel, D. E. McClelland, M. Evans, and N. Mavalvala, Optica **3**, 682 (2016).